Low-lying neutron unbound states in ^{12}Be

J. K. Smith, T. Baumann, D. Bazin, J. Brown, S. Casarotto, P. A. DeYoung, N. Frank, J. Hinnefeld, M. Hoffman, M. D. Jones, Z. Kohley, B. Luther, B. Marks, N. Smith, J. Snyder, A. Spyrou, S. L. Stephenson, M. Thoennessen, N. Viscariello, and S. J. Williams

Phys. Rev. C **90**, 024309 — Published 15 August 2014

DOI: 10.1103/PhysRevC.90.024309

Low-lying neutron unbound states in ^{12}Be

J.K. Smith,[1,2,*] T. Baumann,[1] D. Bazin,[1] J. Brown,[3] S. Casarotto,[4] P.A. DeYoung,[5] N. Frank,[4] J. Hinnefeld,[6] M. Hoffman,[4] M.D. Jones,[1,2] Z. Kohley,[1,7] B. Luther,[8] B. Marks,[5] N. Smith,[4] J. Snyder,[1] A. Spyrou,[1,2] S.L. Stephenson,[9] M. Thoennessen,[1,2] N. Viscariello,[4] and S.J. Williams[1]

[1] *National Superconducting Cyclotron Laboratory, Michigan State University, East Lansing, MI 48824, USA*
[2] *Department of Physics and Astronomy, Michigan State University, East Lansing, MI 48824, USA*
[3] *Department of Physics, Wabash College, Crawfordsville, IN 47933, USA*
[4] *Department of Physics and Astronomy, Augustana College, Rock Island, IL 61201, USA*
[5] *Department of Physics, Hope College, Holland, MI 49422 , USA*
[6] *Department of Physics and Astronomy, Indiana University at South Bend, South Bend, IN 46634, USA*
[7] *Department of Chemistry, Michigan State University, East Lansing, MI 48824, USA*
[8] *Department of Physics, Concordia College, Moorhead, MN 56562, USA*
[9] *Department of Physics, Gettysburg College, Gettysburg, PA 17325, USA*

The neutron decay of an unbound resonance in ^{12}Be has been measured at 1243±21 keV decay energy with a width of 634±60 keV. This state was populated with a one-proton removal reaction from a 71 MeV/u ^{13}B beam incident upon a beryllium target. The invariant mass reconstruction of the resonance was achieved by measuring the daughter fragment in coincidence with neutrons. Despite being above the 2n separation energy, the state decays predominantly by the emission of one neutron to ^{11}Be, setting an upper limit on the branching ratio for the two-neutron decay channel to ^{10}Be of less than 5%. From the characteristics of the population and decay of the resonance, it is concluded that this state cannot correspond to the previously observed state at 4580±5 keV.

PACS numbers: 21.10.-k, 27.20.+n, 29.30.Hs

I. INTRODUCTION

The structure of ^{12}Be has been studied extensively and substantial experimental evidence suggests that the $N = 8$ shell closure, which is present in less exotic $N = 8$ isotopes, is not present in ^{12}Be [1–7]. In addition to the ground state structure, three bound states between 2 and 3 MeV have been measured with spins and parities of 2^+, 0^+, and 1^- [4, 5, 8]. A recent search for an additional 0^- bound state which had been predicted in a three-body model [9, 10] was unsuccessful [11]. Thus, these three states are most likely the complete set of bound states in ^{12}Be. In contrast, very little is known about the level scheme at higher excitation energies, where only two unbound states have been reported below 8 MeV with tentative spin and parity assignments. The states in ^{12}Be, as well as previously measured states in ^{11,10}Be, are shown in Fig. 1.

The lowest-measured unbound excited state in ^{12}Be at 4580 keV is above not only the 1n separation energy, but also the 2n separation energy. It was first measured at an excitation energy of 4559±25 keV in 1978 by Alburger *et al.* with a (t,p) reaction [17]. In 1994, Fortune *et al.* repeated the measurement and reported a resonance energy and width of 4580±5 keV and 107±17 keV, respectively [14]. Since these measurements, the state has been observed with four different reactions: ^{10}Be(^{14}N,^{12}N)^{12}Be, ^{9}Be(^{12}C,^{9}C)^{12}Be, ^{14}C(^{12}C,^{14}O)^{12}Be, and ^{11}Be$(d,p)^{12}$Be [18]. A second unbound excited state was reported at 5700±250 keV [17], 5724±6 keV [14], and 5700 keV [18].

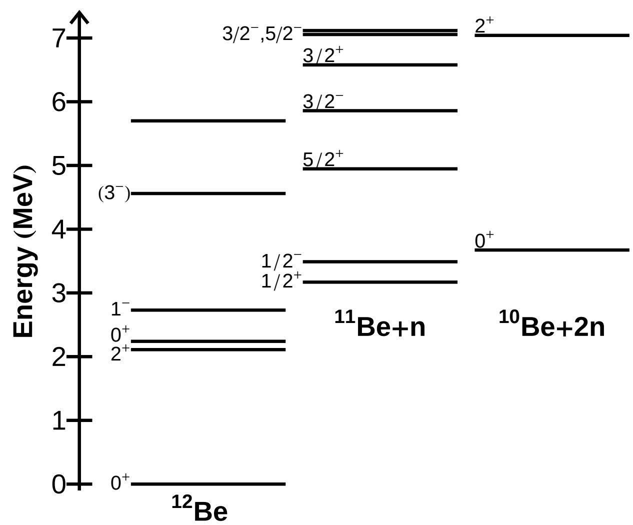

FIG. 1. Level diagram of states in ^{12,11,10}Be, relative to the ground state of ^{12}Be. Neutron separation energies are from [12]. Bound and resonant state energies are from [4, 5, 8, 13–16].

The spin and parity assignment of the first unbound state has been controversial and is presently not resolved. Initially, Fortune *et al.* assigned a spin and parity of 2^+ based on a comparison of angular distribution measurements with DWBA calculations [14]. However, Fortune and Sherr changed that assignment to 3^- based on a private communication from J.D. Millener who suggested that the population of the state was too strong to be a second 2^+ state [19]. In contrast, a recent calculation by

* smithj@nscl.msu.edu

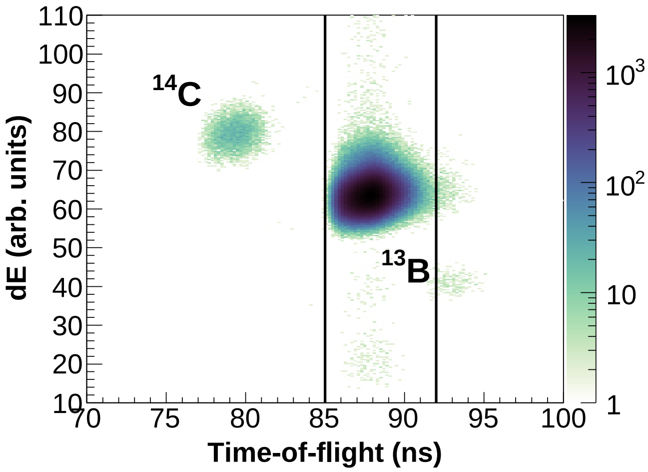

FIG. 2. (Color online) Energy loss measured in the ion chamber versus time-of-flight between timing scintillators for the incoming secondary beam. The lines indicate the gate used to select the ^{13}B beam from the ^{14}C contamination.

Garrido *et al.* suggests a probable spin and parity of 0^+ for this state, although a 1^- or 3^- assignment would also be possible [20, 21]. Garrido's calculations are based on the three-body structure of ^{12}Be and are an extension of previous calculations performed for those bound states [9].

Although the energy and width of the first unbound resonance have been measured, the neutron decay has previously not been observed and the branching ratios to the two bound states in ^{11}Be and the ground state of ^{10}Be have not yet been calculated. This paper reports on the observation of the neutron decay of a low-lying unbound state in ^{12}Be and preliminary limits on its branching ratios. Neutrons were measured in coincidence with ^{11}Be and ^{10}Be fragments to determine the 1n and 2n decay branches.

II. EXPERIMENT

The experiment was carried out at the National Superconducting Cyclotron Laboratory. An ^{18}O primary beam was accelerated through the Coupled Cyclotron Facility to an energy of 120 MeV/u and impinged upon a 2491 mg/cm^2 beryllium target. From the fragmentation products, the A1900 Fragment Separator [22] selected a 96% pure ^{13}B secondary beam at 71 MeV/u. The primary carbon contaminant was eliminated by gating on the time-of-flight between two scintillators (Fig. 2): one located 1 m upstream from the reaction target and the other located 10 m upstream from that.

The ^{13}B beam entered the experimental area (shown in Fig. 3) at a rate of approximately 8×10^5 particles per second. The secondary beam hit a 51 mg/cm^2 beryllium reaction target. A 1p removal reaction in the target created unbound ^{12}Be, which promptly decayed. Daughter fragments of ^{11}Be and ^{10}Be were deflected 43.3° by the large-gap Sweeper dipole magnet [23], while the neutrons propagated 8 m to the Modular Neutron Array (MoNA) [24] and the Large-area multi-Institutional Scintillator Array (LISA). Each detector array contains 144 2 m x 10 cm x 10 cm plastic scintillator bars with photomultipler tubes coupled to each end to measure the time and position of interactions within the array. The two arrays were placed to allow for detection of higher energy neutrons at larger angles while not sacrificing detector depth along the beam axis.

After the Sweeper dipole magnet, a suite of charged particle detectors were used to measure the position, angle, energy loss, remaining energy, and time-of-flight of the charged daughter fragments. Two cathode-readout drift chambers (CRDCs) [25], separated by 1.55 m, measured the positions of the particles. Energy loss was measured with an ion chamber immediately following the CRDCs. A thin (5 mm) dE plastic scintillator was used to trigger the system readout, measure the time-of-flight of the fragments between it and the upstream scintillators, and provide an additional energy-loss measurement. The remaining energies of the fragments were measured with an array of CsI(Na) crystals.

Elemental identification of the daughter fragments was performed using the energy loss in the ion chamber as well as the energy loss in the thin dE scintillator. To improve the purity of the selected events, both energy loss measurements were used to select the beryllium fragments as shown in Fig. 4. The different beryllium isotopes were separated by time-of-flight after correcting for position and angular correlations introduced by the Sweeper dipole magnet following the procedure detailed in Ref. [26]. The final isotope separation can be seen in Fig. 5. The position information after the Sweeper magnet was used to track each fragment back through the dipole field and obtain its momentum vector before the magnet [27].

The momentum vectors of the neutrons in coincidence with the ^{11}Be fragments were calculated from the locations and times of the interactions in MoNA-LISA. Neutron interactions in MoNA-LISA were separated from background γ-rays by setting a threshold of 1 MeVee for total charge deposited in the detector module as well as a time-of-flight gate that corresponded to prompt neutrons.

Information about the shape of the decay energy spectrum can be obtained from the neutron velocity. For neutrons emitted from an unbound fragment or state, the neutron velocity distribution should be centered around the beam velocity. For large decay energies, neutrons emitted perpendicular to the beam axis will not pass through the gap of the Sweeper magnet while neutrons emitted forward or backward in the center of mass will be detected in MoNA-LISA. This effect will result in apparent peaks in the velocity spectrum at higher/lower beam velocities corresponding to the forward/backward emitted neutrons as shown in Fig. 6. The strong forward

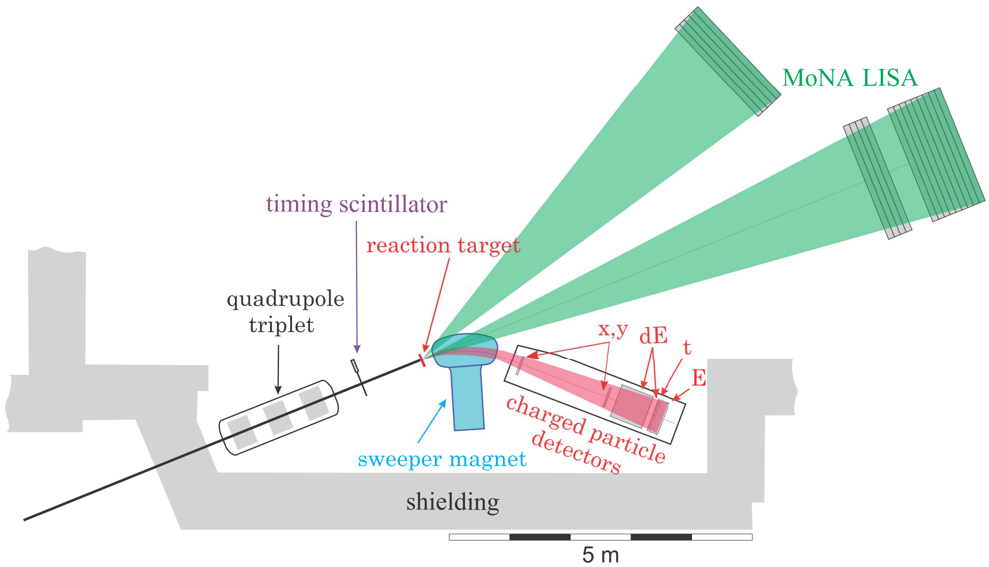

FIG. 3. (Color online) Schematic drawing of the experimental setup.

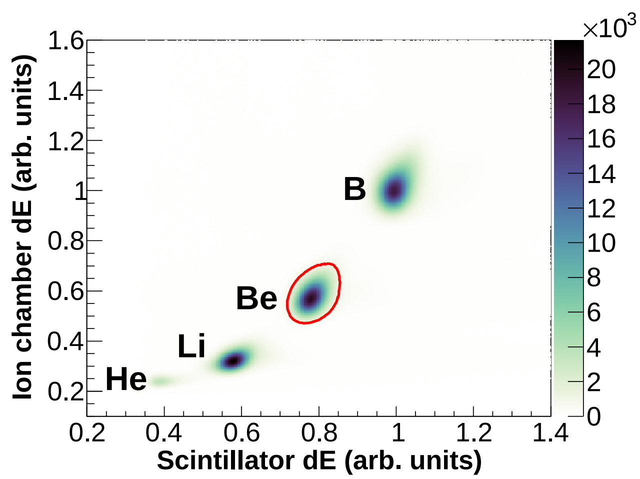

FIG. 4. (Color online) Element identification using the energy loss measurements from the ion chamber (y-axis) and thin scintillator (x-axis). Fragments with $2 \leq Z \leq 5$ were identified. The red contour indicates the beryllium element gate used for this analysis.

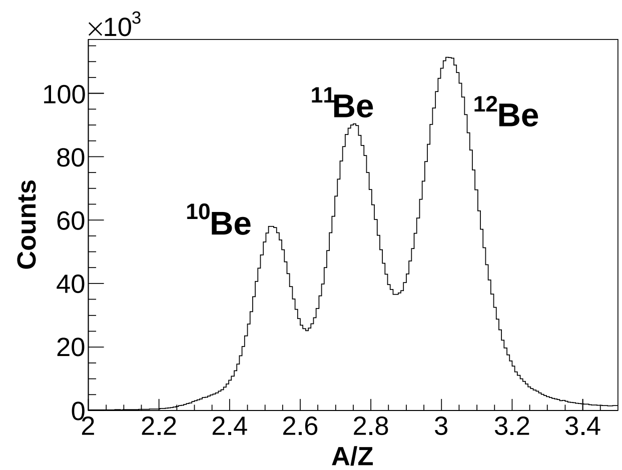

FIG. 5. Beryllium isotopic identification as described in the text.

and backward peaks indicate the presence of a strong resonance at a large energy.

The energy released in the decay of a nucleus to a fragment and one or more (m) neutrons can be calculated using the invariant mass method:

$$E_d = \sqrt{\left(E_f + \sum_{i=1}^{m} E_n\right)^2 - \left(\vec{p}_f + \sum_{i=1}^{m} \vec{p}_n\right)^2} - M_f - mM_n$$

where E_d is the decay energy and $M_{f,n}$, $E_{f,n}$, and $\vec{p}_{f,n}$ are the masses, energies, and momentum vectors of the fragment and neutrons, respectively. For a two-body decay where only one neutron is emitted, this equation can be reduced to:

$$E_d = \sqrt{M_f^2 + M_n^2 + 2(E_f E_n - \vec{p}_f \cdot \vec{p}_n)} - M_f - M_n.$$

The two-body decay energy spectrum for the ^{12}Be→^{11}Be+n decay is shown in Fig. 7. As already evidenced by the neutron velocity spectrum, a strong peak is present around 1200 keV.

The three-body decay of excited ^{12}Be into ^{10}Be+2n is more difficult to measure since a single neutron can interact multiple times in MoNA-LISA and can therefore be incorrectly identified as a two-neutron decay. The interactions in MoNA and LISA were time-ordered and the three-body decay energy spectrum was calculated from the first two interactions. The resulting three-body decay energy spectrum for the ^{12}Be→^{10}Be+2n decay is shown

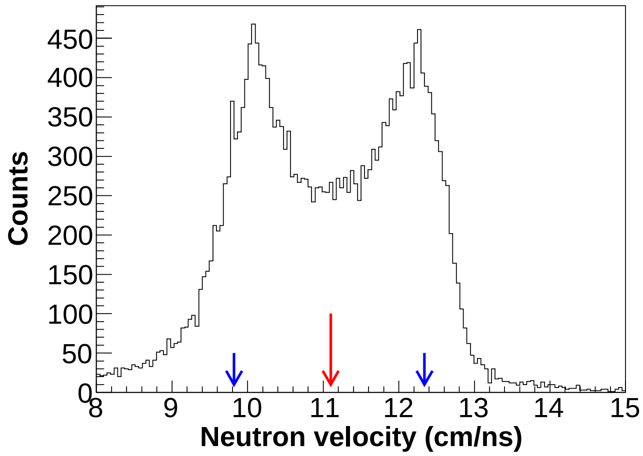

FIG. 6. (Color online) Neutron velocity in coincidence with ^{11}Be fragments. The two peaks show the forward and backward emitted neutrons. The middle red arrow indicates the beam velocity while the two smaller blue arrows indicate the expected velocity for the forward and backward neutrons emitted with a decay energy of 1200 keV.

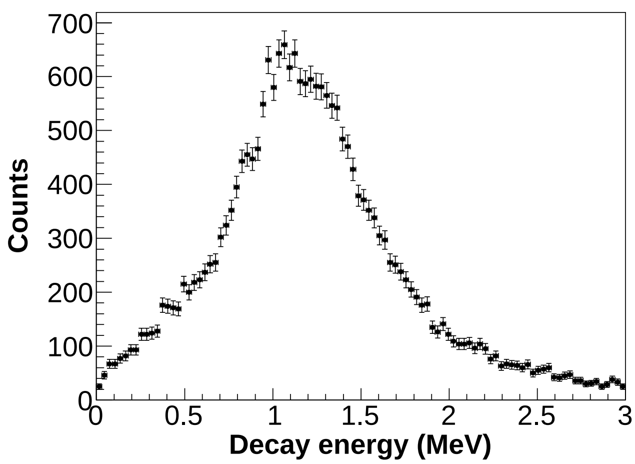

FIG. 7. Two-body decay energy spectrum in coincidence with ^{11}Be fragments.

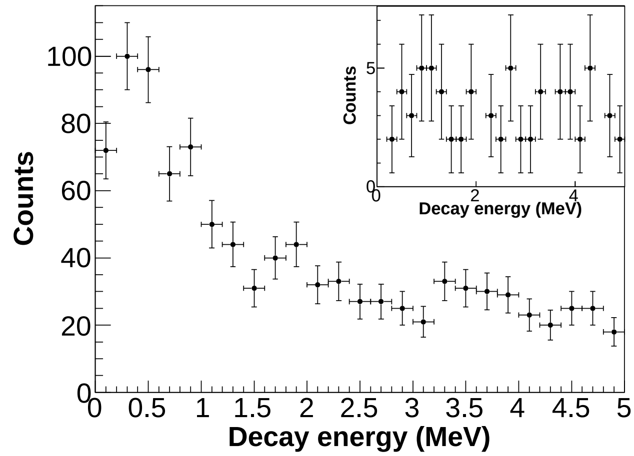

FIG. 8. Three-body (fragment and two neutrons) decay energy spectrum of ^{10}Be in coincidence with two interactions in MoNA-LISA. The data shown in the insert has causality gates applied as explained in the text.

in Fig. 8. This figure still contains incorrectly identified events from a single neutron interacting multiple times. In order to eliminate these events, causality cuts were applied [28–30]. Specifically, the distance between the two interaction points was required to be greater than 50 cm and the velocity of a hypothetical particle traveling between the two interactions had to be greater than the velocity of the neutron traveling from the target to the first interaction point. Although these cuts also eliminate real two-neutron events, they reduce the percent contribution of interactions due to a single neutron scattering. The three-body decay energy spectrum with causality cuts applied is shown in the inset of Fig. 8. The elimination of almost all the events implies that the original three-body spectrum was dominated by one neutron scattering and that the apparent peak around 600 keV does not correspond to a resonance in ^{12}Be.

III. DATA ANALYSIS

The interpretation of the data was performed with a Monte Carlo simulation that includes the incoming beam distribution, the reaction and decay in the target, the neutron-induced interactions in MoNA-LISA, the Sweeper magnet, and all detector resolutions and efficiencies. Modeling of the neutron interactions was performed with GEANT4 and the custom neutron interaction model MENATE_R [31]. The input decay energy lineshape was an energy-dependent Breit-Wigner distribution [32]:

$$\sigma_\ell(E) \propto \frac{\Gamma_\ell}{(E_0 - E + \Delta_\ell)^2 + \frac{1}{4}\Gamma_\ell^2},$$

where the position of the peak is E_0, and the energy-dependent width (Γ_ℓ) and the resonance shift (Δ_ℓ) are both functions of the angular momentum of the neutron (ℓ), the position of the peak, and the intrinsic width of the state (Γ_0). In addition, a small background contribution was simulated with a Maxwellian distribution.

The solid black line in Fig. 9 shows the best fit to the data. It corresponds to an $\ell = 1$ decay with a decay energy of 1243±21 keV and a width of 634±60 keV. A small ($< 2\%$) contribution from a Maxwellian background distribution with an energy of 500 keV is needed to fit the shoulder at low energies. The width compares favorably to the approximately 800 keV single-particle decay width as calculated from Bohr and Mottelson [33]. It was not possible to fit the data with an $\ell = 2$ lineshape simulation unless the width was increased to unphysical

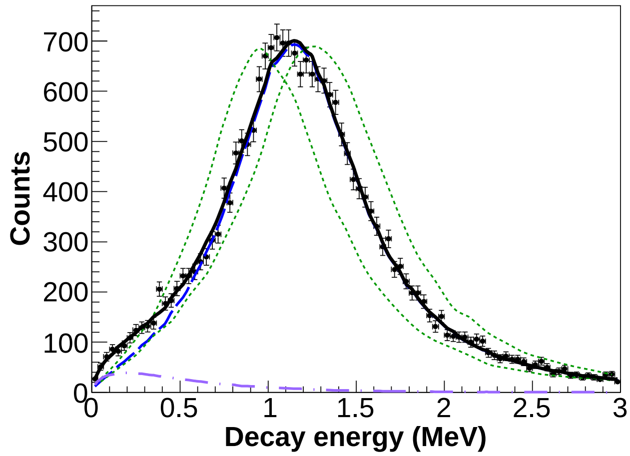

FIG. 9. (Color online) Two-body decay energy spectrum in coincidence with ^{11}Be fragments with the best single decay channel fit. An $\ell = 1$ resonance at an energy of 1243 keV and 634 keV width (blue dashed line) is summed with a Maxwellian background distribution (purple dot-dashed line) for the best fit. The sum is shown by the solid black line. The green dotted lines are explained in Section IV.

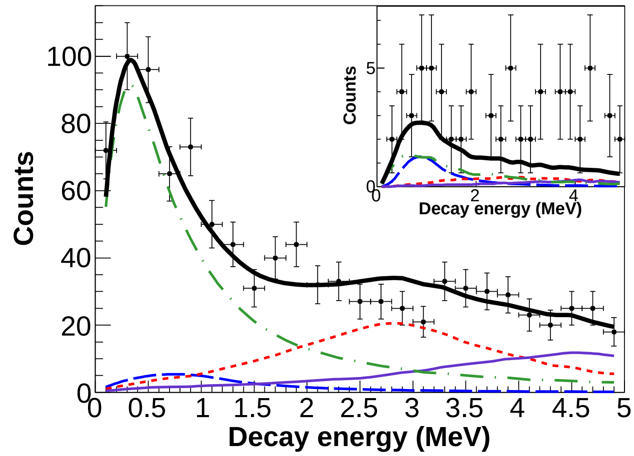

FIG. 10. (Color online) Three-body (fragment and two neutrons) decay energy spectrum of ^{10}Be in coincidence with two interactions in MoNA-LISA. Points are experimental data, while all lines are from simulation. The blue dashed line is a simulation of a two-neutron decay from ^{12}Be. All other colored lines are resonant one-neutron decays from ^{11}Be as used in Ref. [15] and described in the text. The solid black line shows the sum. The inset spectrum shows the same data and simulations with the causality cuts applied.

values of more than 15 times the single-particle width of approximately 250 keV. An $\ell = 0$ resonant state which could be present due to a deformed ^{11}Be core [34, 35] also did not fit the data.

The observed state in ^{12}Be is not only unbound with respect to one-neutron decay but it can also decay to the ground state of ^{10}Be by emitting two neutrons. The measured three-body decay energy spectrum displays a peak at around 500 keV which disappears when the causality cuts are applied (see Fig. 8). The lowest possible excitation energy of the one-neutron decay energy is 4412 keV ($S_n(^{12}\text{Be}) = 3169\pm16$ keV [12]) corresponding to a three-body decay energy of about 740 keV ($S_{2n}(^{12}\text{Be}) = 3671\pm16$ keV [12]). It is therefore unlikely that this state has a significant 2n branching to ^{10}Be. In order to establish an upper limit on the branching ratio of the 2n decay of the ^{12}Be resonance, simulations were performed which (in addition to the 2n decay) included possible contributions from directly populated states in ^{11}Be that subsequently decayed to ^{10}Be. Three unbound states in ^{11}Be that had previously been observed in neutron removal reactions from ^{12}Be [6, 15] were included in the fit: the decay of the $5/2^+$ state and first $3/2^-$ state to the ground state with decay energies of 1277 keV and 2690 keV, respectively, as well as the decay of the second $3/2^-$ state to the first excited state of ^{10}Be ($E_{decay} =$ 80 keV). The resonance parameters taken from Ref. [15] were kept fixed and only the relative intensities of each component were varied.

The results of these simulations displayed in Fig. 10 demonstrate that the spectral shape can be almost completely described with decays from the one-neutron emission from ^{11}Be with only a small contribution from the two-neutron decay of ^{12}Be. In this figure, the blue dashed line is the 2n decay from ^{12}Be, the green dot-dashed line is the decay from the second $3/2^-$ state to the first excited state of ^{10}Be, and the red dotted and purple solid lines correspond to the decays of the $5/2^+$ and $3/2^-$ states to the ground state of ^{10}Be. The effectiveness of the causality cut is shown in the inset plot where most of the cross-talk from multiple interactions of the single neutron decay have been eliminated and only the true two-neutron events remain. The magnitude of the small 2n contribution (as established from the fit to the raw data) is well reproduced. Combining the results of this fit with the strength of the one-neutron decay discussed earlier places an upper limit of 5% on the two-neutron decay branch of the ^{12}Be resonance.

IV. DISCUSSION

The assignment of the observed resonance with a decay energy of 1243±21 keV to an excitation in ^{12}Be is not unique because it can decay to either the $1/2^+$ ground state or the $1/2^-$ first excited state in ^{11}Be. The parity of the initial state can be determined from the multipolarity of the transition ($\ell = 1$) and the parity of the final states. A transition to the positive parity ground state would establish the parity of the ^{12}Be resonance to be negative while a transition to the negative parity first excited state would require the state to be of positive parity. Table I lists the relevant parameters for these two scenarios.

Although neither the $\ell = 0$ nor $\ell = 2$ decays fit the

TABLE I. Parameters for potential decays from positive and negative parity states in ^{12}Be, using S_n=3169±16 keV [12].

	Positive	Negative
Decay energy (keV)	1243±21	1243±21
Multipolarity	$\ell = 1$	$\ell = 1$
Final state $E*$ (keV)	320	0
Final state J^π	$1/2^-$	$1/2^+$
$E* - S_n$	1563±21	1243±21
$E*$	4732±26	4412±26

data, the data can be described by an admixture of $\ell = 1$ and $\ell = 0, 2$ decays. Any $\ell = 0, 2$ contributions would decay to the opposite state as the $\ell = 1$ decay. Thus if the unbound state is of negative (positive) parity, the $\ell = 0, 2$ decay would leave the ^{11}Be daughter in the excited (ground) state and push the central energy of the resonance higher (lower). Therefore the upper and lower limits for the excitation energy of the unbound state are set by the fit with a single $\ell = 1$ component. The range of possible excitation energies is thus from 4400 to 4800 keV.

The 4400 to 4800 keV range might suggest that the currently measured state corresponds to the previously measured 4580 keV state [14]. If this were true, and it decayed by a single channel to the ground or bound excited state in ^{11}Be, the central energy would be 1391 keV or 1071 keV, respectively. Lineshapes with those central energies are shown as the green dotted lines in Fig. 9 and it is evident that they cannot fit the data alone. The strongest argument against the interpretation that these states are identical, however, is the large difference in observed widths. While Fortune *et al.* reported a width of 107±17 keV, the width of the present state is 634±60 keV. Even the empirical enhancement factor of 1.6 suggested in Ref. [36] is not sufficient to explain this discrepancy.

The present data also do not support a 3^- assignment. Any reasonable fits to the data must contain some contribution of $\ell = 1$ decay. Such a decay is forbidden from a 3^- to either the ground or first excited state of ^{11}Be which have spin and parity of $1/2^+$ and $1/2^-$, respectively. The need for the $\ell = 1$ component coupled with the spins and parities of the states in ^{11}Be limits the spin assignment to either 0, 1, or 2. A similar restriction can also be derived from the reaction mechanism. The protons in the $3/2^-$ ground state of ^{13}B predominantly occupy the $s_{1/2}$ and $p_{3/2}$ orbitals. Thus, a one-proton removal reaction can only populate states with spin 0, 1, or 2. The one-proton knockout is also unlikely to populate a 0^- state, since that would require the removal of a $d_{3/2}$ proton.

The above arguments lead to the conclusion that the present experiment populated a new excited state in ^{12}Be with a spin assignment of 0^+, 1^+, 1^-, 2^+, or 2^-. A calculation of neutron decay branching ratios by Garrido

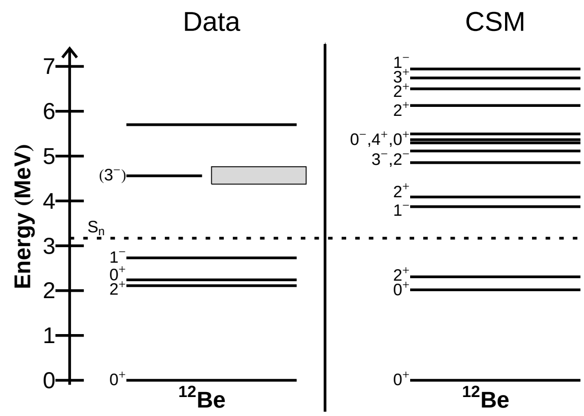

FIG. 11. Level diagram of measured states in ^{12}Be from Fig. 1 and a continuum shell model calculation of states in ^{12}Be [37, 38]. The grey box indicates the bounds for the new state reported in this paper.

et al. [20] shows significant strength to the two neutron decay channel for all calculated positive parity states and much less for all negative parity states. This suggests that the unbound state is either a 1^- or 2^- state.

The observation of a new state does not contradict the original (t, p) measurements. As stated by Fortune *et al.* "Below 6 MeV excitation energy, our data allow us to set an upper limit of 30 μb/sr cross section for any possible missing narrow state of ^{12}Be" [14]. Thus, they were not sensitive to a very broad state as observed in the present experiment.

Additional evidence for a different state can also be deduced from the unpublished work by Johansen [39]. Excited states in ^{12}Be were populated in a (d, p) reaction with a radioactive beam of ^{11}Be in inverse kinematics. A neutron unbound state at an excitation energy of ∼4500 keV was observed. Similar to the present work, the observed width was significantly larger ($\geq$ 200 keV) than the width extracted from the (t, p) experiment (107±17 keV).

A second state in this energy range would resolve the recent disagreement about the spin assignment of the originally measured state between Fortune [40] and Garrido *et al.* [21]. The narrow state observed in the (t, p) reaction could correspond to a 3^- state while the presently observed state could be a 1^- state as proposed by Garrido *et al.* No calculation for a potential unbound state with a spin and parity of 2^- was presented in those reports [20, 21].

The presence of additional states in this energy region is not unexpected. Continuum shell model calculations [37, 38] predict several unbound states including one 2^- and two 1^- as shown in Fig. 11. The lower-lying 1^- state corresponds most likely to the measured bound 1^- state. The 2^- state has a calculated energy most similar to the presently measured state.

V. SUMMARY

In summary, we have measured the neutron decay of an unbound state in ^{12}Be. The one-neutron decay energy spectrum is best fit by an $\ell = 1$ decay with a decay energy of 1243±21 keV. This corresponds to an excitation energy of either 4412 keV or 4732 keV depending on the final state of the fragment and to a range of 4400 to 4800 keV when the possibility of simultaneous decay to the ground and excited states of ^{11}Be are considered. The extracted width is 634±60 keV. No evidence for the 2n decay channel to ^{10}Be was observed, establishing an upper limit of 5% for this decay branch. Although the measured excitation energy is consistent with the previously measured state at 4580 keV, the large width as well as the small 2n branching ratio indicate that this is a new state. Based on the measured branching ratios, the selectivity of the reaction mechanism, and comparison to theory, the most likely spin and parity for this new state is 2^-.

ACKNOWLEDGMENTS

The authors would like to thank all the members of the MoNA Collaboration, especially Paul Gueye and Joe Finck for their detailed feedback on the original manuscript. This work was funded by NSF grant PHY-1102511. The construction of LISA was funded by the following NSF grants: PHY-0922794, PHY-0922473, PHY-0922446, PHY-0922537, PHY-0922462, PHY-0922409, PHY-0922335, PHY-0922622, PHY-0969058 and PHY-0969173. This material is based upon work supported by the Department of Energy National Nuclear Security Administration under Grant No. DE-NA0000979 and DOE Grant No. DE-FG02-92ER40750.

[1] F. Nunes, J. Christley, I. Thompson, R. Johnson, and V. Efros, Nucl. Phys. A **609**, 43 (1996).
[2] A. Navin *et al.*, Phys. Rev. Lett. **85**, 266 (2000).
[3] H. Iwasaki *et al.*, Phys. Lett. B **481**, 7 (2000).
[4] H. Iwasaki *et al.*, Phys. Lett. B **491**, 8 (2000).
[5] S. Shimoura *et al.*, Phys. Lett. B **560**, 31 (2003).
[6] S. D. Pain *et al.*, Phys. Rev. Lett. **96**, 032502 (2006).
[7] R. Meharchand *et al.*, Phys. Rev. Lett. **108**, 122501 (2012).
[8] D. E. Alburger, D. P. Balamuth, J. M. Lind, L. Mulligan, K. C. Young, R. W. Zurmühle, and R. Middleton, Phys. Rev. C **17**, 1525 (1978).
[9] C. R. Romero-Redondo, E. Garrido, D. V. Fedorov, and A. S. Jensen, Phys. Rev. C **77**, 054313 (2008).
[10] C. Romero-Redondo, E. Garrido, D. V. Fedorov, and A. S. Jensen, Phys. Lett. B **660**, 32 (2008).
[11] J. G. Johansen *et al.*, Phys. Rev. C **88**, 044619 (2013).
[12] "ENSDF," (2011).
[13] S. Shimoura *et al.*, Phys. Lett. B **654**, 87 (2007).
[14] H. T. Fortune, G.-B. Liu, and D. E. Alburger, Phys. Rev. C **50**, 1355 (1994).
[15] W. A. Peters *et al.*, Phys. Rev. C **83**, 057304 (2011).
[16] J. Kelley, E. Kwan, J. Purcell, C. Sheu, and H. Weller, Nucl. Phys. A **880**, 88 (2012).
[17] D. E. Alburger, S. Mordechai, H. T. Fortune, and R. Middleton, Phys. Rev. C **18**, 2727 (1978).
[18] H. G. Bohlen, W. Von Oertzen, T. Z. Kokalova, C. H. Schulz, R. Kalpakchieva, T. Massey, and M. Milin, Int. J. Mod. Phys. E **17**, 2067 (2008).
[19] H. T. Fortune and R. Sherr, Phys. Rev. C **83**, 044313 (2011).
[20] E. Garrido, A. S. Jensen, D. V. Fedorov, and J. G. Johansen, Phys. Rev. C **86**, 024310 (2012).
[21] E. Garrido, A. S. Jensen, D. V. Fedorov, and J. G. Johansen, Phys. Rev. C **88**, 039802 (2013).
[22] D. Morrissey, B. Sherrill, M. Steiner, A. Stolz, and I. Wiedenhoever, Nucl. Instruments Methods Phys. Res. Sect. B Beam Interact. with Mater. Atoms **204**, 90 (2003).
[23] M. Bird, S. Kenney, J. Toth, H. Weijers, J. DeKamp, M. Thoennessen, and A. Zeller, IEEE Trans. Appiled Supercond. **15**, 1252 (2005).
[24] B. Luther *et al.*, Nucl. Instruments Methods Phys. Res. Sect. A Accel. Spectrometers, Detect. Assoc. Equip. **505**, 33 (2003).
[25] J. Yurkon, D. Bazin, W. Benenson, D. Morrissey, B. Sherrill, D. Swan, and R. Swanson, Nucl. Instruments Methods Phys. Res. Sect. A Accel. Spectrometers, Detect. Assoc. Equip. **422**, 291 (1999).
[26] G. Christian *et al.*, Phys. Rev. C **85**, 034327 (2012).
[27] N. Frank, A. Schiller, D. Bazin, W. Peters, and M. Thoennessen, Nucl. Instruments Methods Phys. Res. Sect. A Accel. Spectrometers, Detect. Assoc. Equip. **580**, 1478 (2007).
[28] C. R. Hoffman *et al.*, Phys. Rev. C **83**, 031303(R) (2011).
[29] E. Lunderberg *et al.*, Phys. Rev. Lett. **108**, 142503 (2012).
[30] Z. Kohley *et al.*, Phys. Rev. C **87**, 011304 (2013).
[31] Z. Kohley *et al.*, Nucl. Instruments Methods Phys. Res. Sect. A Accel. Spectrometers, Detect. Assoc. Equip. **682**, 59 (2012).
[32] A. M. Lane and R. G. Thomas, Rev. Mod. Phys. **30**, 257 (1958).
[33] A. Bohr and B. R. Mottelson, *Nuclear Structure*, Vol. 1 (W.A. Benjamin, Inc., 1969).
[34] J. L. Lecouey, Few-Body-Systems **34** (2004), 10.1007/s00601-004-0029-3.
[35] I. Hamamoto and S. Shimoura, J. Phys. G Nucl. Part. Phys. **34**, 2715 (2007).
[36] H. T. Fortune, Nucl. Instruments Methods Phys. Res. Sect. A Accel. Spectrometers, Detect. Assoc. Equip. **681**, 7 (2012).
[37] A. Volya and V. Zelevinsky, Phys. Rev. C **74**, 064314 (2006).
[38] A. Volya, (2014), private communication.

[39] J. G. Johansen, *Transfer reaction study of neutron rich beryllium isotopes*, Ph.D. thesis, Aarhus University (2012).

[40] H. T. Fortune, Phys. Rev. C **88**, 039801 (2013).